Sensors and Actuators A 154 (2009) 212–217

Contents lists available at ScienceDirect

Sensors and Actuators A: Physical

journal homepage: www.elsevier.com/locate/sna

Optimization of an electromagnetic comb drive actuator

S. Schonhardt [a,*], J.G. Korvink [a], J. Mohr [b], U. Hollenbach [b], U. Wallrabe [a]

[a] University of Freiburg – IMTEK, Department of Microsystems Engineering, Freiburg, Germany
[b] Forschungszentrum Karlsruhe GmbH, IMT Institut für Mikrostrukturtechnik, Germany

ARTICLE INFO

Article history:
Received 27 March 2008
Received in revised form 31 July 2008
Accepted 1 August 2008
Available online 20 August 2008

Keywords:
Electromagnetic
Actuator
Optimization
System stability
Comb drive
Magnetic properties

ABSTRACT

We present the first electromagnetic comb drive actuator which allows for over 100 μm of linear actuator motion at large air gap widths of 25 μm at 300 coil windings, a structural height of 400 μm and for an applied current of 8 mA. Previously reported designs require very narrow air gaps of 3 μm at structural heights of up to 1 mm [K. Fischer, H. Guckel, Long throw linear magnetic actuators stackable to one millimeter of structural height, Microsyst. Technol., 4 (1998) 180–183] which makes them sensitive to operate, and challenging to fabricate. The new design reduces the reluctance by a parallel connection and cascading of several pole shoes as is well known for electrostatic actuators. This reduces the current consumption and linearizes the current–displacement characteristic. The cascaded design further enhances the displacement range at the cost of a slightly increased current consumption at the onset of the stroke. To analyze the influence of the number of air gaps on the plunger motion the total cross-sectional area of the magnetic core is kept constant while the number of air gaps is varied. Magnetic and mechanical material properties are measured for an accurate simulation of the system behavior. Experimental results confirm the theoretical predictions.

1. Introduction

Most actuators which are found in the literature for micro-scaled applications are of the capacitive type [2–4]. Electromagnetic actuators, however, excel by higher achievable energy densities and can be reasonably operated with relatively large air gap widths in comparison to electrostatic actuators [5,6]. This makes them more powerful, less sensitive to environmental dust particles and simpler to control since high voltages are not required. The maximal achievable actuator forces are limited only by material saturation and heat generation within the driving coils. Recently published electromagnetic actuators can be classified into three basic types according to their air gap configuration (Fig. 1).

The first type features facing pole shoes in a serial configuration, where the distance between the two faces changes with displacement [6,7]. This set-up shows classical pull-in behavior at 1/3 of its maximum displacement when connected to a spring, as is known for the switch point of electromagnetic relays. This behavior drastically limits the controllable range and is commonly used when large contact forces are required. The second type features parallel pole shoes in a serial configuration, where the overlap area changes with displacement. This allows for a continuous plunger displacement at moderate current consumption [1,6]. Type III actuators feature both characteristics. The overlap area as well as the gap distance changes with displacement. The pole shoe geometry has a large influence on the actuator performance [8]. This paper analyzes this influence, which leads to a new type of actuator featuring several type II actuators connected in parallel, and which resembles an electrostatic comb drive (Fig. 2).

2. Circuit model

The behavior of the three air gap types is described by a network model, where each air gap is represented by a displacement dependent reluctance R_{Gap} under the assumption that the material permeability $\mu_r \gg 1$ and consequently all magnetic field lines remain within the ferromagnetic core, so that the actuator can be represented by a network model in analogy to an electrical circuit model using Kirchhoff's basic laws [6,9] (Fig. 3). Table 1 shows the correspondence between magnetic and electrical circuits.

Stator and plunger can thus be treated like lumped parameter resistors and the two air gaps as displacement dependent variable resistors. The resistance depends upon the geometric shape (l represents the length and A the cross-sectional area) and the permeability μ of the constituent material (1).

$$R(x) = \frac{l(x)}{\mu A(x)} \tag{1}$$

* Corresponding author.
E-mail address: Stefan.Schonhardt@imtek.de (S. Schonhardt).

0924-4247/$ – see front matter © 2008 Elsevier B.V. All rights reserved.
doi:10.1016/j.sna.2008.08.007

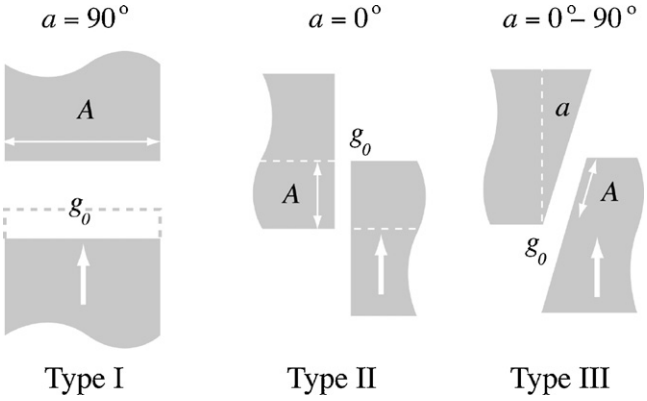

Fig. 1. Basic pole shoe geometries. g_0 represents the initial displacement and A represents the overlap area.

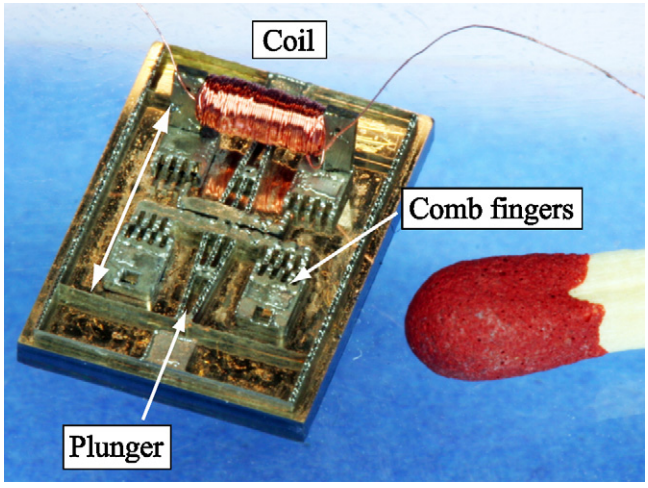

Fig. 2. Magnetic comb drive actuator made of nickel–iron (78/22) in a LIGA process with $N = 2$ and 8 air gaps. One externally wound coil is removed for better visibility. The chip width is 8000 μm.

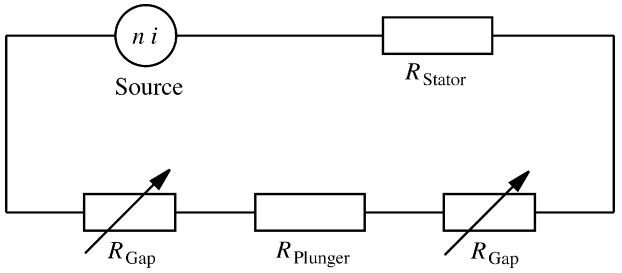

Fig. 3. Network model of a serial magnetic actuator with two displacement dependent air-gap reluctances R_{Gap} and the core reluctances $R_{Plunger}$ and R_{Stator}.

Table 1
Correspondence between magnetic and electric circuits

Electric	Magnetic
Voltage, V	Magnetomotive force $\theta = nI$
Current, I	Magnetic flux $\phi = \theta/R_{Gap}(x)$
Resistance, R	Reluctance $R_{Mag} = l/\mu A$

n represents the number of coil windings, l the length of the magnetic path, A the cross-sectional area of the magnetic path and μ the magnetic permeability.

Table 2
Displacement dependent reluctance $R_{Gap}(x)$ of the three basic pole shoe geometries

Type	Reluctance	Characteristic
I	$R_I \sim \frac{g_0 - x}{A}$	Linear, small displacement, pull-in instability
II	$R_{II} \sim \frac{g_0^2}{x}$	Inverse law, large displacement, small air gap, stable
III	$R_{III} = \beta R_I + \gamma R_{II}$	Combined, large displacement, large initial air gap

A represents the overlap area and g_0 the gap width in the initial position. The influence of types I and II can be adjusted via the inclination angle for type III as is represented by β and γ.

The actuator force (3) can then be calculated from the total energy contained in the system via the total inductance (2). We use the principle of *virtual displacement*.

$$L(x) = \frac{n^2}{R_{Core} + R_{Gap}(x)} \tag{2}$$

$$F = \frac{1}{2} i^2 \frac{\partial}{\partial x} \left(\frac{n^2}{R_{Core} + R_{Gap}(x)} \right) \tag{3}$$

The integer n is the number of coil windings and i the driving current. To generate large actuation forces the displacement-dependent derivative of the total inductance in (3) has to be maximized. The term depends upon the reciprocal of the constant core reluctances ($R_{Plunger}$ and R_{Stator}) as well as the displacement-dependent reluctances $R_{Gap}(x)$ (2). A strong change of the reluctance $R_{Gap}(x)$ with respect to x corresponds to a high actuator force for this displacement. This is usually achieved by a small air gap width g_0 ($l(x)$ in Eq. (1)), which would render fabrication a difficult task. The inductance difference between the initially open and the completely closed air gaps defines the maximum achievable actuation force. Consequently, the constant core reluctances have to be of a low value.

3. Air gap classification

The differing behavior of the basic air gap shapes as shown in Fig. 1 can be clearly explained by their different reluctance characteristics as is given in Table 2.

For type I actuators the reluctance linearly decreases with displacement and the overlap area A can be used as a tuning parameter. This causes the total inductance L to increase over the whole displacement range (2) causing strongly rising actuation forces (3). This leads to system instability as will be explained in more detail in the following section. For type II actuators $R_{Gap}(x)$ decreases inversely with the displacement, causing large actuation forces for small displacements x, which rapidly fade out. The system shows stability over the whole stroke. The gap width g_0 can be used for tuning within the fabrication limits. The inclined pole shoe faces of type III actuators represent a combination of type I and II incorporating both characteristics (Fig. 1), since the gap width g_0 as well as the overlap area A change with displacement. The respective influences on the total reluctance can be expressed by β and γ, which in turn depends on the inclination angle α [8].

4. Stability examination

For a deeper understanding of the system and to avoid plunger pull-in for type III actuators in future designs the point of instability is analyzed. At the pull-in point two conditions hold:

Force equilibrium between the actuator and the opposing suspension spring:

$$\frac{\partial W^*_{Ges}}{\partial x} = 0 \Rightarrow kx - \frac{1}{2} i^2 \frac{\partial L(x)}{\partial x} = 0 \tag{4}$$